



Contents lists available at ScienceDirect

Physics Letters A

www.elsevier.com/locate/pla

Perpetual points and hidden attractors in dynamical systems

Dawid Dudkowski^{a,*}, Awadhesh Prasad^b, Tomasz Kapitaniak^a

^a Division of Dynamics, Technical University of Lodz, Stefanowskiego 1/15, 90-924 Lodz, Poland

^b Department of Physics and Astrophysics, University of Delhi, Delhi 110007, India

ARTICLE INFO

Article history:

Received 18 April 2015

Received in revised form 30 May 2015

Accepted 1 June 2015

Available online xxxx

Communicated by C.R. Doering

Keywords:

Perpetual points

Co-existing hidden attractors

Forced systems

ABSTRACT

We discuss the use of perpetual points for tracing the hidden and the rare attractors of dynamical systems. The analysis of perpetual points and their co-existence due to the parameters values is presented and the impact of these points on the behavior of the systems is shown. The results are obtained for single as well as coupled externally excited van der Pol–Duffing oscillators. The presented results can be generalized to other systems having different dynamics.

© 2015 Elsevier B.V. All rights reserved.

1. Introduction

The theory of nonlinear dynamical systems is one of the fastest growing branches of applied mathematics, which is nowadays used in many areas of physics, chemistry and other natural sciences. The possible final states of the system – known as its attractors – are the key concept of this theory. Recently, new types of attractors known as the *hidden* [1–15] and *rare* [16–21] are thoroughly studied.

The hidden attractors – the ones whose basins of attraction do not intersect with the neighborhood of any equilibrium, have been found in Chua's circuit [1–4], Lorenz type systems [5–7], chaotic flows [8–11] and others. In [12] the authors study a time-delayed system, and in [13] hidden oscillations of autonomous van der Pol–Duffing oscillator are described. In the control theory [4,14] this type of states is also analyzed. Thorough study on the topic can be found in [15], where Leonov and Kuznetsov investigate the hidden attractors from the very beginning of this phenomenon.

The second lately described type of states are the rare attractors – these, whose basins of attraction are significantly smaller than the basins of other co-existing attractors (so their occurrence is less probable and localization is not straightforward) [16]. The concept of rare attractors was introduced by Zakrzhevsky et al. in [17], where mechanical system with several degrees of freedom is discussed. In [18–20] studies about different types of pendulum systems can be found and in [21] the authors describe rare attractors in discrete-time models.

The concepts of the described two types of attractors are not identical and define quite different kinds of states. An attractor can be a hidden one but not rare and vice versa. The hidden property depends on the existence (and location) of equilibria in the system, which cannot be changed without interfering with the parameters or the structure of the system itself. On the other hand, the attractor can be considered as rare depending on the set of accessible initial conditions [16]. Nonetheless, in many models (especially the ones without any equilibria), attractors can be simultaneously hidden and rare. The examples of such attractors are presented in our research.

Multistability in dynamical system is a common feature. Uncovering all co-existing attractors and their basins are very important for understanding the systems. One of the major difficulties in understanding such systems is to locate the co-existing attractors. This becomes even more difficult when these states are either hidden or rare. In this paper we attempt to locate such hidden/rare attractors which co-exist in a large number even in simple examples.

The most elementary analysis of dynamical systems usually begins from searching for stationary points of the system and studying their stability. Although the theory of the fixed points (equilibria) is very well known [22–26], many interesting results can still be obtained [27–35]. Stochastic equations [27], fractional-order models [28], Hamiltonian systems [29], equations with delays [27, 30,31] are only a few examples of the issues for which the studies about stationary points are still being carried out. Due to the nature of the hidden and rare attractors the stationary points are much less useful for tracking such states, than they are for the systems with self-excited attractors.

* Corresponding author.

E-mail address: dawid.dudkowski@p.lodz.pl (D. Dudkowski).

In this work we investigate the new class of critical points, called *perpetual points*, which have been introduced by Prasad in [36]. These are defined as the points where the acceleration of the system becomes zero while velocity remains nonzero. Various interesting properties of these points and their use can be found in the quoted paper.

In order to present the results we consider a van der Pol–Duffing oscillator, which is one of the most studied dynamical systems [37–53]. The bifurcation analyses of this system (including e.g., Hopf, Hopf–Pitchfork bifurcations) can be found in [37–43]. In [43] the influence of the noise on the dynamics is presented, while in [44,45] the impact of two external forces is shown. Many studies refer to the adaptive synchronization of the oscillators [46,47], different types of coupling [40,48], delay feedback [37,49–51]. Some analytical considerations can be found in [52], while in [53–55] different types of attractors are studied. All these works confirm that the van der Pol–Duffing system is the issue for which many interesting results have been obtained and many more can still be done.

In this paper we use the perpetual points to locate the hidden/rare attractors. Their analysis and the influence on the dynamics are studied and discussed. Section 2.1 contains the main results obtained for a single oscillator, while in Section 2.2 the results for the coupled systems are shown. Conclusions are presented in Section 3.

2. Results

2.1. Single oscillator

We consider single externally excited van der Pol–Duffing oscillator which is given by equation

$$\ddot{x} - \alpha(1 - x^2)\dot{x} + x^3 = F \sin(\omega t), \quad (1)$$

where x is the state variable and α, F and ω are constant parameters. In all calculations in this subsection we have fixed the first two parameters at $\alpha = 0.2$ and $F = 1$. For various ω values the system (1) can be monostable (e.g., for $\omega = 0.8$) having one self-excited attractor, as well as multistable, in which case the hidden and self-excited attractors co-exist. Considering suitable phase space boundaries, some of these attractors are also rare.

In order to find perpetual points, system (1) has to be transformed into a set of first-order autonomous ordinary differential equations (as the result the phase space will be three-dimensional) and the second derivatives of the state variables of such system have to be equal to zero.

We denote x_1 as the position variable ($x_1 := x$) and x_2 as the velocity ($x_2 := \dot{x}$), while t is considered as the new, time-dependent variable (which obviously appears as the equation $\dot{t} = 1$). Consequently, perpetual points of the system (1) are solutions of the set of equations:

$$\begin{cases} \alpha(1 - x_1^2)x_2 - x_1^3 + F \sin(\omega t) = 0 \\ -2\alpha x_1 x_2^2 - 3x_1^2 x_2 + \omega F \cos(\omega t) = 0. \end{cases} \quad (2)$$

Relation (2) consists of polynomial equations (due to the variables x_1, x_2) and is underdetermined – 2 equations with 3 variables. We have been searching for the perpetual points in the box $(x_1, x_2, t) \in [-2, 2] \times [-3, 3] \times [0, 2\pi/\omega]$, for fixed value of ω . The boundaries for position and velocity variables result from the basins of attraction of system (1), where initial conditions of rare attractors are mostly located. The structure of these basins is complicated [12] and changes mainly due to the value of ω parameter. The examples and analysis of these rare attractors can be found in [16]. On the other hand, periodicity of trigonometric functions present in (1) implicates the boundary for t .

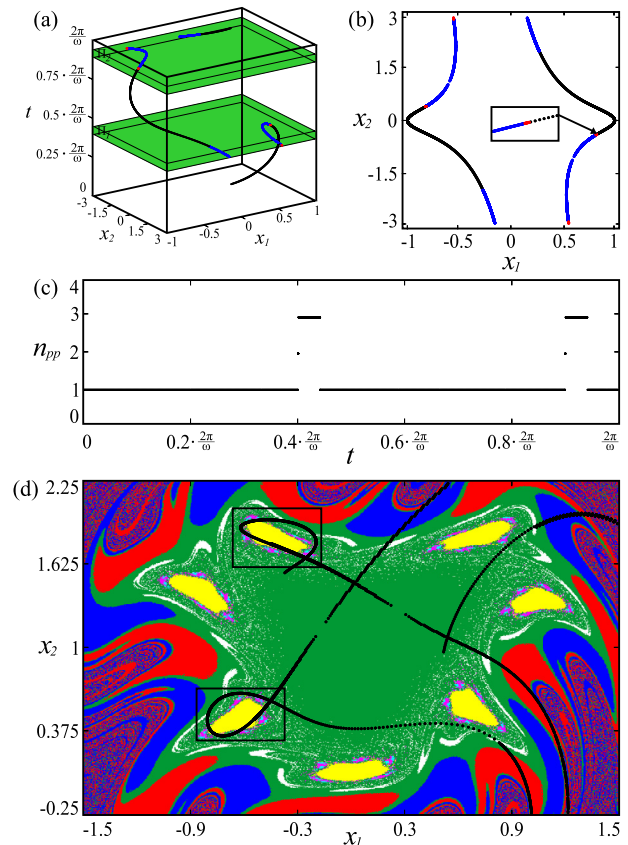


Fig. 1. (Color online.) Perpetual points of system (1) for parameter $\omega = 0.962$. In (a) points in three-dimensional phase space (x_1, x_2, t) are shown, while in (b) their projection on (x_1, x_2) plane is presented. (c) The number of co-existing points as a function of time. (d) The basins of attraction for single oscillator and the trajectory points (marked as black dots) when crossing the $t = 2\pi/\omega$.

Relation (2) can be transformed into one rational equation due to variable x_1 and solved for fixed t . In our calculations the Newton's method for finding approximations to the function roots is used. Also, the form of equations in (2) allows to observe a simple property, that is helpful in finding the perpetual points, i.e., if the point (x_1^*, x_2^*, t^*) , where $t^* \in [0, T/2]$ for $T := 2\pi/\omega$ is perpetual one, then the point $(-x_1^*, -x_2^*, t^* + T/2)$ is perpetual too. This fact allows to reduce the searching to interval $t \in [0, T/2]$. Nonetheless, both points (x_1^*, x_2^*, t^*) and $(-x_1^*, -x_2^*, t^* + T/2)$ should be examined for the attractors because due to the asymmetry of basins of attraction they may lead to different states.

The results of our calculations for $\omega = 0.962$ are shown in Fig. 1. The existence of perpetual points in three-dimensional phase space (x_1, x_2, t) is presented in Fig. 1(a). Each element of the curves represents the perpetual point obtained for relation (2) for fixed t value. The position of these points changes continuously when t increases. The phase space is splitted into three parts – the blank region and two subspaces Π_1 and Π_2 marked as green boxes. In the blank one, for a fixed t only one perpetual point exists and is unique on (x_1, x_2) plane. In Π_1 and Π_2 spaces one observes co-existence of the perpetual points. For fixed t we have two co-existing points (marked as red dots) or three co-existing points (marked as blue ones) as shown in Fig. 1(a–b). The intervals of t values where this co-existence appears are presented in Fig. 1(c), where n_{pp} denotes number of perpetual points. As one can observe, there are two narrow time intervals for $n_{pp} = 2$ and two wider for $n_{pp} = 3$. For better clarity, in Fig. 1(b) the projection of the obtained points on (x_1, x_2) plane is shown. The color code corresponds to Fig. 1(a) and part of the curve where co-existence appears is shown as an enlargement in the inset. The symmetry

of the figure around point $(0,0)$ results from the above described property of equations (2). In order to determine the attractors to which the obtained points lead when considered as initial conditions for (1), we have run the system from each one of them and have saved the space coordinates when trajectory crosses fixed surface – $t = 2\pi/\omega$. The obtained results are shown in Fig. 1(d). The basins of attraction for $t = 2\pi/\omega$ (which changes periodically with the period of excitation of system (1)) have been used as the background of the plot. Each color correspond to the basin of different attractor. The dynamics of each state is determined using Poincare sections, based on the period of external excitation. The number of the points on the map corresponds to the periodicity of solution. In the considered example, the red, blue and green basins are the dominant ones and refer to two 9 periodic and a quasiperiodic attractor respectively. The other states, for space boundaries as in the figure, can be considered as the rare attractors – their occurrence for randomly chosen initial conditions is significantly less probable than for the dominating attractors. The white region leads to a 25 periodic solution and the pink one to a state of period 35. In the area marked by cyan color two 70 periodic attractors co-exist, though, due to the applied resolution and limitations of calculations, their basins are not separated. Similarly in the yellow region, where three possible solutions can be obtained – two symmetrical 49-periodic and 63-periodic one. For the considered value of parameter ω one unstable fixed point exists, i.e., $(x_1, x_2) = (0, 0)$, and its neighborhood intersects with the basin of quasiperiodic solution (green region). Thus, by definition, the quasiperiodic attractor is self-excited and the remaining attractors (periodic ones) are hidden.

Trajectory points when crossing $t = 2\pi/\omega$ surface are marked as black dots in Fig. 1(d). As one can notice, the points cross various regions, also the ones where rare attractors basins are located (the examples of these are marked as two black insets in Fig. 1(d)). This implies the diversity of the observed states. Using perpetual points we have obtained ten attractors for the considered system – nine periodic and one quasiperiodic.

The results obtained for different values of ω are presented in Fig. 2. In the left panel, Figs. 2(a–d), the projections of Poincare maps of system (1) on the x_1 subspace are shown. For each perpetual point taken as the initial condition (points are identified by t value on the horizontal axis and in the case of the co-existing points only one of them is considered), the map is calculated and its projection is plotted on the vertical axis of the diagram. Such results allow to analyze the type and the number of the co-existing attractors, e.g., for (a) $\omega = 0.955$ and (b) $\omega = 0.963$ the irregular attractors (chaotic or quasiperiodic) can be observed and also the periodic ones, most of them of high period. On the other hand, when ω increases, for (c) $\omega = 0.966$ and (d) $\omega = 0.972$ only regular dynamics is present and the period of possible solutions has decreased. Knowing the initial conditions (perpetual points), we can also trace these attractors and locate some approximations of their basins of attraction. Using the same method of calculations, in the right panel – Figs. 2(e–f), the behavior of the states obtained for various values of ω parameter is shown. Each color on the plot corresponds to the period of the solution obtained for fixed ω and the perpetual point (calculated for corresponding t value). In Fig. 2(e) high period solutions are presented, while in Fig. 2(f), the low period ones are shown. It should be emphasized that for some attractors values of their period are off the scale. Such a situation occurs when the dynamics is quasiperiodic or chaotic (for these we denote 150 on the color scale; the highest period we have observed is 148) and when the behavior is periodic indeed, but the period value is lower or higher than the boundary of the color code which is actually used (e.g., some of the attractors in Fig. 2(e) are below period 50, but are denoted by color corresponding to this value). Nevertheless, from the obtained results

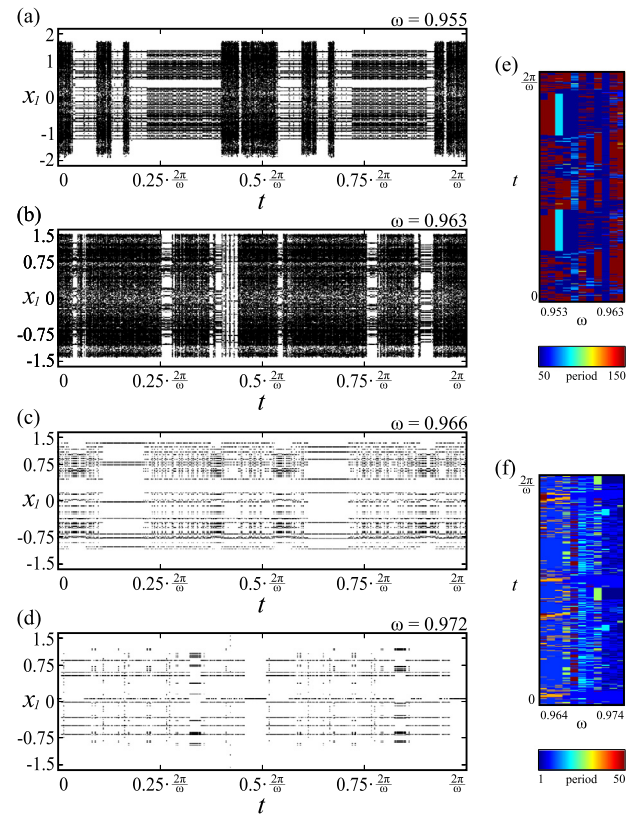


Fig. 2. (Color online.) In the left panel – (a–d), different types of attractors of system (1), obtained for calculated perpetual points, are shown as the projections of their Poincare maps on the x_1 subspace. Increasing from the top to the bottom, $\omega = 0.955, 0.963, 0.966, 0.972$ respectively. In the right panel – (e–f), period of solutions is shown, with (e) corresponding to $\omega \in [0.953, 0.963]$ and (f) corresponding to $\omega \in [0.964, 0.974]$.

one can conclude how complex the dynamics of system (1) is and how it changes, even for slightly different parameter values. Even though the position of perpetual points in space changes continuously with t , we can observe essential differences in the character of the solutions to which these points lead. This gives an idea of how irregular boundaries of basins of co-existing attractors are.

2.2. Coupled oscillators

In this subsection we consider a system of two coupled externally excited van der Pol–Duffing oscillators which is given by equations

$$\begin{cases} \ddot{x} - \alpha(1 - x^2)\dot{x} + x^3 + g_1(x, y, \dot{x}, \dot{y}) = F \sin(\omega t) \\ \ddot{y} - \alpha(1 - y^2)\dot{y} + y^3 + g_2(x, y, \dot{x}, \dot{y}) = F \sin(\omega t), \end{cases} \quad (3)$$

where x, y are the state variables, α, F, ω are the parameters and g_1, g_2 are the coupling functions. In all our calculations we have fixed the parameters for both oscillators at $\alpha = 0.2, F = 1$ and $\omega = 0.962$. The coupling functions can be chosen arbitrarily and in peculiar cases they can depend on both the position and the velocity of the oscillators. In our considerations these functions have been defined as $g_1 = \varepsilon(y - x)$ and $g_2 = \varepsilon(x - y)$, where $\varepsilon \geq 0$ is the coupling coefficient and can be read as linear springs that couple oscillators.

The method of finding perpetual points of system (3) is the same as it is for the previous equation (1). Here, we denote x_1 as the position and x_2 as the velocity of the first oscillator (first equation in (3)), y_1 as the position and y_2 as the velocity of the second oscillator (second equation in (3)) and t as the new

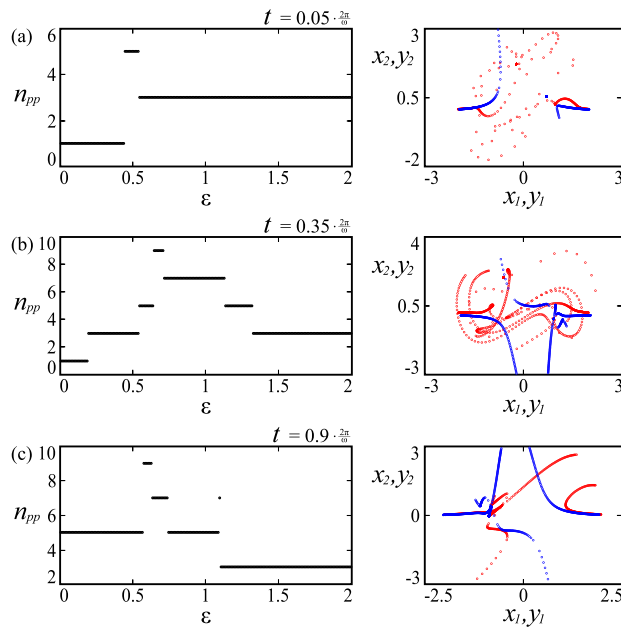


Fig. 3. (Color online.) Number of co-existing perpetual points (n_{pp} parameter) in the function of coupling strength ε (left panel) and projection of these points on position-velocity plane (blue dots in right panel) for system (3). Variable t is fixed for each diagram and increases from the top to the bottom, $t = 0.05 \cdot 2\pi/\omega$, $0.35 \cdot 2\pi/\omega$, $0.9 \cdot 2\pi/\omega$ respectively. Points of trajectories (starting from perpetual points) while crossing the $t = 2\pi/\omega$ surface are marked as red dots.

time-dependent variable. Perpetual points of the system (3) are the solutions of the set of equations:

$$\begin{cases} \alpha(1 - x_1^2)x_2 - x_1^3 + F \sin(\omega t) + \varepsilon(x_1 - y_1) = 0 \\ -2\alpha x_1 x_2^2 - 3x_1^2 x_2 + \omega F \cos(\omega t) + \varepsilon(x_2 - y_2) = 0 \\ \alpha(1 - y_1^2)y_2 - y_1^3 + F \sin(\omega t) + \varepsilon(y_1 - x_1) = 0 \\ -2\alpha y_1 y_2^2 - 3y_1^2 y_2 + \omega F \cos(\omega t) + \varepsilon(y_2 - x_2) = 0. \end{cases} \quad (4)$$

Likewise, relation (4) consists of polynomial equations (due to the variables x_1, x_2, y_1, y_2) and is underdetermined – 4 equations of 5 variables. The area of searching for perpetual points is analogous as in the case of a single oscillator – five-dimensional phase space $(x_1, x_2, y_1, y_2, t) \in [-2, 2] \times [-3, 3] \times [-2, 2] \times [-3, 3] \times [0, 2\pi/\omega]$. Although, due to the coupling components, equations (4) can be simplified into two polynomial equations due to variable x_1, x_2 (or y_1, y_2 , which depend on the transformation) and then solved for fixed t . In calculations, the version of Newton's method for solving nonlinear systems of equations is used.

Relation (4) has the same property as relation (2), i.e., if point $(x_1^*, x_2^*, y_1^*, y_2^*, t^*)$, where $t^* \in [0, T/2]$ for $T := 2\pi/\omega$ is perpetual one, then point $(-x_1^*, -x_2^*, -y_1^*, -y_2^*, t^* + T/2)$ is perpetual too. Moreover, due to the similarity of equations (4) and (2) and from the fact that oscillators are identical, two additional observations can be made. Firstly, if (x_1^*, x_2^*, t^*) is a perpetual point of system (1), then the point $(x_1^*, x_2^*, x_1^*, x_2^*, t^*)$ is a perpetual point of system (3) for any value of the coupling coefficient ε (the coupling components disappear). Secondly, for a fixed value of ε , if $(x_1^*, x_2^*, y_1^*, y_2^*, t^*)$ is a perpetual point of system (3), then the point $(y_1^*, y_2^*, x_1^*, x_2^*, t^*)$ is also a perpetual point of system (3) (which concludes from the symmetry of equations (1, 3) and (2, 4) in (4)). The knowledge of these properties allows to optimize the calculations.

The results of our research are shown in Fig. 3. In the left panel, the number of the obtained perpetual points in the function of coupling strength is presented. For each plot t variable is fixed and the number of points, denoted by n_{pp} parameter, has been calculated for $\varepsilon \in [0, 2]$. As one can observe, when $t = 0.05 \cdot 2\pi/\omega$

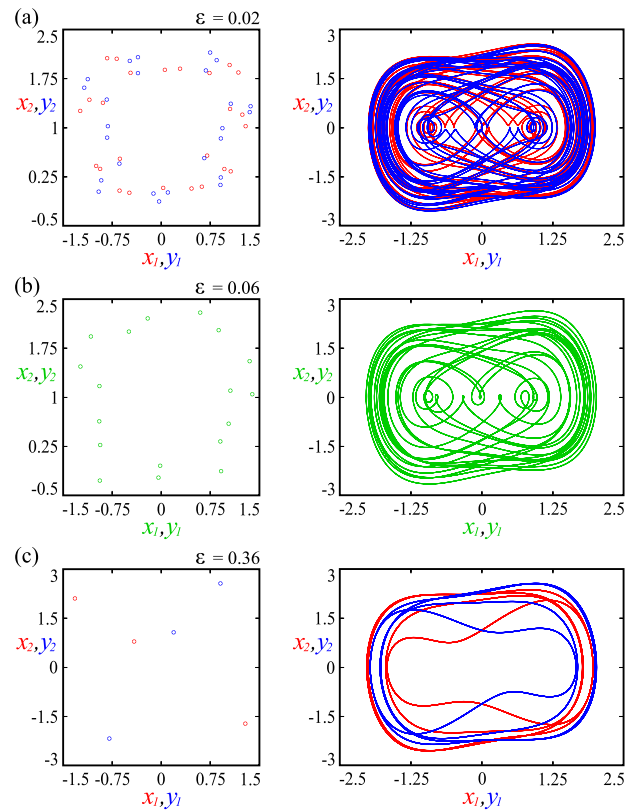


Fig. 4. (Color online.) Poincaré maps (left) and trajectories (right) of regular attractors obtained from perpetual points, that exist only for coupled oscillators system (3). Increasing from the top to the bottom, $\varepsilon = 0.02$ (co-existing attractors of period 25), $\varepsilon = 0.06$ (one common attractor of period 18) and $\varepsilon = 0.36$ (co-existing attractors of period 3).

(Fig. 3(a)), for small coupling perpetual points are unique, then when the strength increases, in the narrow interval 5 points co-exist and after reaching some threshold ε value, n_{pp} parameter stabilizes on 3. For larger t values, Fig. 3(b–c), more complex behavior occurs and the number of co-existing points varies. For $t = 0.35 \cdot 2\pi/\omega$ it changes from 1 to 9 and for $t = 0.9 \cdot 2\pi/\omega$ from 3 to 9. It should be noted that the n_{pp} parameter is even in all these cases. It is a simple conclusion from the properties of relation (4) described above. For all t values considered in Fig. 3, the single system (1) has one unique perpetual point and for every point obtained for the coupled system there co-exists the corresponding point if we interchange the oscillators. Hence, $n_{pp} = 1 + 2k$ for some $k \in \mathbb{N}$. In the right panel in Fig. 3 the corresponding projections of perpetual points on position-velocity plane are marked as blue dots. The position of points in phase space (on curves) changes continuously with increasing t , like it is for a single oscillator. In addition, we plot the trajectory points of system (3) when they cross fixed subspace $t = 2\pi/\omega$ and these points are presented as red dots in figure.

Considering the perpetual points as the initial conditions one can obtain the attractors that appear only for the coupled system (3) and have not been found for a single oscillator (1), for the same parameter values (the attractors of single van der Pol-Duffing model for parameters $\alpha = 0.2$, $F = 1$ and $\omega = 0.962$ can be found in [54]). The examples of these states are shown in Fig. 4 and Fig. 5. In both figures Poincaré maps are presented in the left panel and the projections of trajectories on two-dimensional plane in the right one. The colors on the plots correspond to the legend on the axes (the oscillators first – x , and the second – y are denoted by red and blue colors respectively). The only exception is Fig. 4(b), where both subsystems are marked in green.

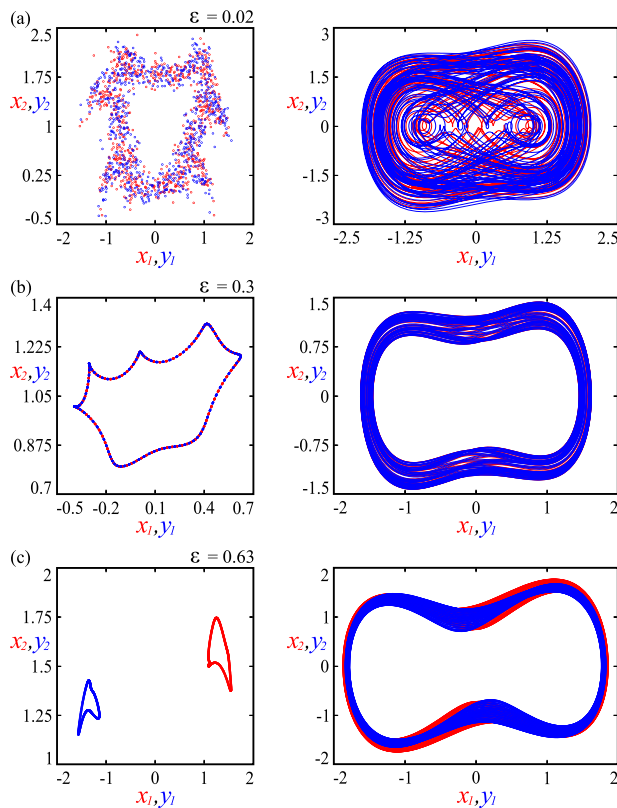


Fig. 5. (Color online.) Poincaré maps (left) and trajectories (right) of irregular attractors obtained from perpetual points, that exist only for coupled oscillators system (3). Increasing from the top to the bottom, $\varepsilon = 0.02$ (co-existing chaotic attractors), $\varepsilon = 0.3$ (one common quasiperiodic attractor) and $\varepsilon = 0.63$ (co-existing quasiperiodic attractors).

In Fig. 4 the examples of periodic solutions are presented, for fixed coupling parameter values. In Fig. 4(a) two states of period 25 co-exist. The trajectories are symmetric around the origin of coordinate systems and the oscillators are anti-phase synchronized. The example of synchronization is shown in Fig. 4(b), where both subsystems get attracted to the 9 period solution. Another anti-phase synchronization scenario is presented in Fig. 4(c), where the value of attractors period is 3. On the other hand, irregular attractors for coupled systems are shown in Fig. 5. An example of chaotic one is in Fig. 5(a). Though the oscillators are desynchronized, the attractors seem to have similar structure. In Figs. 5(b–c), the quasiperiodic dynamics is presented. In the first, the subsystems are synchronized with a lag on one common state. In the second one, oscillators are anti-phase synchronized on two tori. Any state shown in Figs. 4–5 (in the sense of attractor on which the first or the second oscillator is) have not been observed for a single system using perpetual points. It suggests that these states can be born only when the oscillators are coupled.

The results obtained for the coupled system can be generalized in two ways. Any number of oscillators can be considered, which complicates the equations to solve, although, in the case of the simple coupling functions like the one used in the above example, the system can still be simplified into two polynomial equations and two-dimensional Newton's method can be used. Also, different types of coupling functions can be studied.

3. Conclusions

In this work we have given numerical evidence showing that the perpetual points are useful in finding and describing the hidden and rare attractors in the dynamical systems, both single and

the coupled ones. In the first case, the discussed points allow to trace the co-existing attractors of multistable systems and optimize the issue. Instead of analyzing the entire phase space (usually high-dimensional) it is enough to examine the perpetual points – which are usually finite or low-dimensional set (in our example one-dimensional curves). This suggests that we can minimize the computational time for searching as well as accurately uncovering the co-existing attractors. In the coupled system, though, the study of perpetual points allows us to identify new local behavior of the oscillators, that has not been seen for a single unit. Since any of the obtained attractors (red, blue or green in Figs. 4–5) have not been found for a single oscillator, it is not easy to determine the initial conditions for which they can be born for the coupled subsystems using standard methods. All presented results can be successfully obtained also for other systems, both single and coupled, with different types of dynamics.

Further studies of the complex structure of the basins of attraction of the perpetual points and the basins of corresponding attractors can lead to the better understanding of the connection between perpetual points and hidden attractors.

Described results show that, despite its simplicity, the van der Pol–Duffing oscillator is very rich in terms of dynamics and that each study on this system provides new and interesting results. Furthermore, presented technique of application of perpetual points may be very useful to analyze and understand the complicated behavior of such systems, which can extend our knowledge in the theory of nonlinear dynamical systems.

Acknowledgement

This work has been supported by the Polish National Science Centre, MAESTRO Programme – Project No. 2013/08/A/ST8/00/780.

References

- [1] G.A. Leonov, N.V. Kuznetsov, V.I. Vagaitsev, *Physica D* 241 (2012) 1482.
- [2] G.A. Leonov, N.V. Kuznetsov, V.I. Vagaitsev, *Phys. Lett. A* 375 (2011) 2230.
- [3] Q. Li, H. Zeng, X.-S. Yang, *Nonlinear Dyn.* 77 (2014) 255.
- [4] V.O. Bragin, V.I. Vagaitsev, N.V. Kuznetsov, G.A. Leonov, *J. Comput. Syst. Sci. Int.* 50 (2011) 511.
- [5] Z. Wei, R. Wang, A. Liu, *Math. Comput. Simul.* 100 (2014) 13.
- [6] C. Li, J.C. Sprott, *Int. J. Bifurc. Chaos Appl. Sci. Eng.* 24 (2014) 1450034.
- [7] G.A. Leonov, N.V. Kuznetsov, T.N. Mokaev, *arxiv:1505.04729v1 [nlin.CD]*.
- [8] M. Molaie, S. Jafari, J.C. Sprott, S.M.R.H. Golpayegani, *Int. J. Bifurc. Chaos Appl. Sci. Eng.* 23 (2013) 1350188.
- [9] V.-T. Pham, S. Jafari, C. Volos, X. Wang, S.M.R.H. Golpayegani, *Int. J. Bifurc. Chaos Appl. Sci. Eng.* 24 (2014) 1450146.
- [10] S. Jafari, J. Sprott, *Chaos Solitons Fractals* 57 (2013) 79.
- [11] S. Jafari, J. Sprott, S.M.R.H. Golpayegani, *Phys. Lett. A* 377 (2013) 699.
- [12] U. Chaudhuri, A. Prasad, *Phys. Lett. A* 378 (2014) 713.
- [13] H. Zhao, Y. Lin, Y. Dai, *Int. J. Bifurc. Chaos Appl. Sci. Eng.* 24 (2014) 1450080.
- [14] N.V. Kuznetsov, G.A. Leonov, S.M. Seledzhi, in: *Preprints of the 18th IFAC World Congress, Milano (Italy), August 28–September 2, 2011*.
- [15] G.A. Leonov, N.V. Kuznetsov, *Int. J. Bifurc. Chaos Appl. Sci. Eng.* 23 (2013) 1330002.
- [16] A. Chudzik, P. Perlikowski, A. Stefanski, T. Kapitaniak, *Int. J. Bifurc. Chaos Appl. Sci. Eng.* 21 (2011) 1907.
- [17] M. Zakrzhevsky, I. Schukin, V. Yevstignejev, *Transport and Engineering – Mechanics*, 2007–24.
- [18] M. Zakrzhevsky, A. Klovov, V. Yevstignejev, E. Shilvan, A. Kragis, in: *7th International DAAAM Baltic Conference 'Industrial Engineering', 22–24 April 2010, Tallinn, Estonia*.
- [19] A.V. Klovov, M.V. Zakrzhevsky, *Int. J. Bifurc. Chaos Appl. Sci. Eng.* 21 (2011) 2825.
- [20] A. Klovov, M. Zakrzhevsky, in: *Proceedings of the 2nd International Symposium on Rare Attractors and Rare Phenomena in Nonlinear Dynamics, Latvia, Riga – Jurmala, 16–20 May 2011*.
- [21] V. Yevstignejev, A. Klovov, R. Smirnova, I. Schukin, in: *4th IEEE International Conference on Nonlinear Science and Complexity, August 6–11, 2012, Budapest, Hungary*.
- [22] D.J. Higham, T. Sardar, *Appl. Numer. Math.* 18 (1995) 155.
- [23] H. Fujisaka, T. Yamada, *Prog. Theor. Phys.* 69 (1983) 1240.

- [24] M. Shensa, IEEE Trans. Circuit Theory 18 (1973) 481.
- [25] E.K. Blum, X. Wang, Neural Netw. 5 (1992) 577.
- [26] L.G. Khazin, E.E. Shnol, Stability of Critical Equilibrium States, Nonlinear Science: Theory and Applications, vol. XII, Manchester University Press, Manchester/New York, 1991, 208 pp.
- [27] J. Luo, J. Math. Anal. Appl. 334 (2007) 431.
- [28] E. Ahmed, A.M.A. El-Sayed, H.A.A. El-Saka, J. Math. Anal. Appl. 325 (2007) 542.
- [29] H.E. Cabral, K.R. Meyer, Nonlinearity 12 (1999) 1351.
- [30] B. Zhang, Nonlinear Anal. 63 (2005) e233.
- [31] C. Jin, J. Luo, Proc. Am. Math. Soc. 136 (2008) 909.
- [32] T.A. Burton, Nonlinear Anal. 61 (2005) 857.
- [33] T.A. Burton, T. Furumochi, Dyn. Syst. Appl. 10 (2001) 89.
- [34] S.T. Kingni, S. Jafari, H. Simo, P. Wofo, Eur. Phys. J. Plus 129 (2014) 1.
- [35] V.-T. Pham, C. Volos, S. Jafari, Z. Wei, X. Wang, Int. J. Bifurc. Chaos Appl. Sci. Eng. 24 (2014) 1450073.
- [36] A. Prasad, Int. J. Bifurc. Chaos Appl. Sci. Eng. 25 (2015) 1530005.
- [37] S. Ma, Q. Lu, Z. Feng, J. Math. Anal. Appl. 338 (2008) 993.
- [38] J.C. Ji, J. Sound Vib. 297 (2006) 183.
- [39] A. Algaba, E. Freire, E. Gamero, A.J. Rodriguez-Luis, Nonlinear Dyn. 16 (1998) 369.
- [40] A.P. Kuznetsov, J.P. Roman, Physica D 238 (2009) 1499.
- [41] A. Algaba, E. Freire, E. Gamero, A.J. Rodriguez-Luis, Nonlinear Dyn. 22 (2000) 249.
- [42] U.E. Vincent, B.R. Nana Nbandjo, A.A. Ajayi, A.N. Njah, P.V.E. McClintock, Int. J. Dyn. Control (2015), <http://dx.doi.org/10.1007/s40435-014-0118-1>.
- [43] K.R. Schenk-Hoppe, Nonlinear Dyn. 11 (1996) 255.
- [44] F.M. Moukam Kakmeni, S. Bowong, C. Tchawoua, E. Kaptoum, J. Sound Vib. 277 (2004) 783.
- [45] Z. Jing, Z. Yang, T. Jiang, Chaos Solitons Fractals 27 (2006) 722.
- [46] H.B. Fotsin, P. Wofo, Chaos Solitons Fractals 24 (2005) 1363.
- [47] H. Fotsin, S. Bowong, J. Daafouz, Chaos Solitons Fractals 26 (2005) 215.
- [48] A.P. Kuznetsov, N.V. Stankevich, L.V. Turukina, Physica D 238 (2009) 1203.
- [49] X. Li, J.C. Ji, C.H. Hansen, C. Tan, J. Sound Vib. 291 (2006) 644.
- [50] A. Maccari, J. Sound Vib. 317 (2008) 20.
- [51] J. Xu, K.W. Chung, Physica D 180 (2003) 17.
- [52] A. Kimiaefar, A.R. Saidi, G.H. Bagheri, M. Rahimpour, D.G. Domairry, Chaos Solitons Fractals 42 (2009) 2660.
- [53] W. Szemplinska-Stupnicka, J. Rudowski, J. Sound Vib. 199 (1997) 165.
- [54] D. Dudkowski, P. Kuzma, T. Kapitaniak, Discrete Dyn. Nat. Soc. (2014).
- [55] P. Kuzma, M. Kapitaniak, T. Kapitaniak, J. Theor. Appl. Mech. 52 (2014) 281.